Gazi Üniversitesi
Fen Bilimleri Dergisi
PART C: TASARIM VE TEKNOLOJİ

Gazi University
Journal of Science
PART C: DESIGN AND TECHNOLOGY

GU J Sci, Part C, 13(2): 567-578 (2025)

Tailoring the Optical and Electrical Properties of ZnO Films: Co-Doping with F and In

Ibrahim GUNES[1,2*]

[1]*Çanakkale Onsekiz Mart University, Canakkale Faculty of Applied Sciences, Department of Energy Management, Çanakkale, Turkey*

[2]*Çanakkale Onsekiz Mart University, Biga Vocational School, Department of Electricity and Energy, Çanakkale, Turkey*

Article Info

Research article
Received: 18/01/2025
Revision: 04/03/2025
Accepted: 05/03/2025

Keywords

Ultrasonic Spray Pyrolysis
TCO Materials
F:In Co-doped ZnO
Optical Properties
Electrical Properties

Makale Bilgisi

Araştırma makalesi
Başvuru: 18/01/2025
Düzeltme: 04/03/2025
Kabul: 05/03/2025

Anahtar Kelimeler

Ultrasonik Sprey Piroliz
TCO Malzemeler
F:In Eş-katkılı ZnO
Optik Özellikler
Elektriksel Özellikler

Graphical/Tabular Abstract (Grafik Özet)

In this study, undoped ZnO (ZO), In-doped ZnO (IZO), and F:In co-doped ZnO (FIZO) films were synthesized via ultrasonic spray pyrolysis (USP). The F:In co-doping strategy significantly improved structural, optical, and electrical properties, enhancing their potential for opto-electronic applications. / Bu çalışmada katkısız ZnO (ZO), In katkılı ZnO (IZO) ve F:In eş-katkılı ZnO (FIZO) filmleri ultrasonik sprey pirolizi (USP) yöntemiyle sentezlendi. F:In eş-katkılama stratejisi, yapısal, optik ve elektriksel özellikleri önemli ölçüde iyileştirerek opto-elektronik uygulamalar için potansiyelini artırdı.

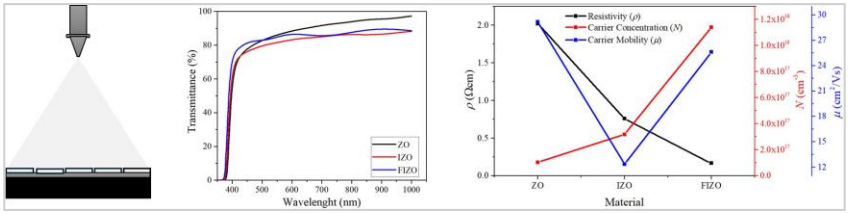

***Figure A**: Schematic of the film deposition process (left), transmittance spectra (middle), and change of electrical parameters (right) / **Şekil A:** Film biriktirme sürecinin şeması (sol), geçirgenlik spektrumları (orta) ve elektriksel parametrelerin değişimi (sağ)*

Highlights (Önemli noktalar)

- *F:In co-doping strategy significantly enhances the opto-electronic properties of ZnO films. / F:In eş-katkılama stratejisi, ZnO filmlerinin opto-elektronik özelliklerini önemli ölçüde geliştirir.*
- *FIZO films exhibit improved carrier concentration and lower electrical resistivity. / FIZO filmleri, daha yüksek taşıyıcı konsantrasyonu ve daha düşük elektriksel özdirenç sergiler.*
- *Optical transmittance (~83%) and wider band gap (3.32 eV) make FIZO films suitable for opto-electronic applications. / Optik geçirgenlik (~%83) ve geniş bant aralığı (3.32 eV), FIZO filmlerini opto-elektronik uygulamalar için uygun hale getirir.*

***Aim (Amaç):** To investigate the impact of F:In co-doping on the structural, optical, and electrical properties of ZnO films and enhance their applicability in opto-electronic devices. / ZnO filmlerinde F:In eş-katkılamanın yapısal, optik ve elektriksel özellikler üzerindeki etkisini inceleyerek opto-elektronik cihazlardaki uygulanabilirliğini artırmak.*

***Originality (Özgünlük):** This study provides a comprehensive analysis of the effects of F:In co-doping in ZnO films synthesized via USP, a rarely explored method, and demonstrates significant improvements in opto-electronic performance. / Bu çalışma, literatürde az çalışılan USP yöntemiyle sentezlenen ZnO filmlerinde F:In eş katkılama etkilerini kapsamlı şekilde inceleyerek opto-elektronik performanstaki önemli gelişmeleri ortaya koymaktadır.*

***Results (Bulgular):** F:In co-doping altered the ZnO crystal structure, leading to enhanced electrical conductivity and optical transparency. The carrier concentration in FIZO films increased 11-fold, resistivity decreased to 1.65×10^{-1} Ωcm, and optical transmittance reached ~83%. / F:In eş-katkılama, ZnO kristal yapısını değiştirerek elektriksel iletkenlik ve optik geçirgenliği artırmıştır. FIZO filmlerinde taşıyıcı konsantrasyonu 11 kat artmış, özdirenç 1.65×10^{-1} Ωcm'ye düşmüş ve optik geçirgenlik ~%83'e ulaşmıştır.*

***Conclusion (Sonuç):** The findings confirm that F:In co-doping effectively improves the structural and opto-electronic properties of ZnO films. With high transparency, enhanced conductivity, and an optimized figure of merit, FIZO films present strong potential for photovoltaic, display, and LED technologies. / Bulgular, F:In eş-katkılamanın ZnO filmlerinin yapısal ve opto-elektronik özelliklerini etkin bir şekilde iyileştirdiğini doğrulamaktadır. Yüksek geçirgenlik, artırılmış iletkenlik ve optimize edilmiş performans faktörü ile FIZO filmleri, fotovoltaik, görüntüleme ve LED teknolojileri için güçlü bir potansiyel sunmaktadır.*

*Corresponding author, e-mail: ibrahimgunes@comu.edu.tr
DOI: 10.29109/gujsc.1622733

GU J Sci, Part C, 13(2): 567-578 (2025)

Gazi Üniversitesi
Fen Bilimleri Dergisi
PART C: TASARIM VE TEKNOLOJİ

Gazi University
Journal of Science
PART C: DESIGN AND TECHNOLOGY

http://dergipark.gov.tr/gujsc

Tailoring the Optical and Electrical Properties of ZnO Films: Co-Doping with F and In

Ibrahim GUNES[1,2*]

[1]*Çanakkale Onsekiz Mart University, Canakkale Faculty of Applied Sciences, Department of Energy Management, Çanakkale, Turkey*

[2]*Çanakkale Onsekiz Mart University, Biga Vocational School, Department of Electricity and Energy, Çanakkale, Turkey*

Article Info

Research article
Received: 18/01/2025
Revision: 04/03/2025
Accepted: 05/03/2025

Keywords

Ultrasonic Spray Pyrolysis
TCO Materials
F:In Co-doped ZnO
Optical Properties
Electrical Properties

Abstract

In this study, undoped ZnO, 3% In doped ZnO and 5% F: 3% In co-doped ZnO films were successfully synthesized via ultrasonic spray pyrolysis. The study objective is to investigate the changes in physical properties –especially opto-electrical– of ZnO films with F:In co-doping strategy and thus contribute to developing high-performance materials for opto-electronic devices. Structural analysis showed that obvious changes occurred in the ZnO crystal structure with doping and the dopant atoms were successfully integrated into the ZnO lattice. Morphological studies showed that 5% F: 3% In co-doped ZnO films exhibit a homogeneous, nanostructured, and compact surface, with surface roughness being lower than undoped ZnO films. Moreover, SEM images identified granular nanostructures in 3% In doped and 5% F: 3% In co-doped ZnO films, which were attributed to the stabilization of grain boundaries by dopant atoms, promoting a uniform structure. Optical analysis revealed that the 5% F: 3% In co-doped ZnO film exhibited a transmittance of 83% in the visible region and a wider optical band gap of 3.32 eV compared to other films. Electrical characterization demonstrated that the carrier concentration of ZnO films was 1.03×10^{17} cm^{-3}, increasing markedly to 1.14×10^{18} cm^{-3} in 5% F: 3% In co-doped ZnO film. Additionally, the resistivity of the 5% F: 3% In co-doped ZnO film was detected at the lowest level of 1.65×10^{-1} Ωcm. This data reveals the potential of 5% F: 3% In co-doped ZnO films for advanced opto-electronic applications, including photovoltaic cells, display technologies, and LEDs. Co-doping ZnO films with fluorine and indium emerge as a promising strategy to enhance electrical and optical properties.

ZnO Filmlerin Optik ve Elektriksel Özelliklerinin Düzenlenmesi: F ve In ile Eş-Katkılama

Makale Bilgisi

Araştırma makalesi
Başvuru: 18/01/2025
Düzeltme: 04/03/2025
Kabul: 05/03/2025

Anahtar Kelimeler

Ultrasonik Sprey Piroliz
TCO Malzemeler
F:In Eş-katkılı ZnO
Optik Özellikler
Elektriksel Özellikler

Öz

Bu çalışmada, katkısız ZnO, %3 In katkılı ZnO ve %5 F: %3 In eş-katkılı ZnO filmleri ultrasonik sprey pirolizi ile başarıyla sentezlendi. Çalışmanın amacı, F:In eş-katkılama stratejisi ile ZnO filmlerinin fiziksel özelliklerindeki (özellikle opto-elektriksel) değişimleri incelemek ve böylece opto-elektronik cihazlar için yüksek performanslı malzemeler geliştirmeye katkıda bulunmaktır. Yapısal analiz, katkılama ile ZnO kristal yapısında belirgin değişimler meydana geldiğini ve katkı atomlarının ZnO örgüsüne başarıyla entegre olduğunu göstermiştir. Morfolojik çalışmalar, %5 F: %3 In eş-katkılı ZnO filmlerinin homojen, nanoyapılı ve kompakt bir yüzey sergilediğini, yüzey pürüzlülüğünün katkısız ZnO filmlerinden daha düşük olduğunu göstermiştir. Dahası, SEM görüntüleri, katkı atomları tarafından tane sınırlarının stabilizasyonuna atfedilen ve düzgün bir yapıyı destekleyen %3 In katkılı ve %5 F: %3 In eş katkılı ZnO filmlerinde granüler nanoyapıları tanımladı. Optik analiz, %5 F: %3 In eş-katkılı ZnO filminin görünür bölgede %83'lük bir geçirgenlik ve diğer filmlere kıyasla 3.32 eV'lik daha geniş bir optik bant aralığı sergilediğini ortaya koydu. Elektriksel karakterizasyon, ZnO filmlerinin taşıyıcı konsantrasyonunun 1.03×10^{17} cm^{-3} olduğunu, %5 F: %3 In eş-katkılı ZnO filminde 1.14×10^{18} cm^{-3}'e belirgin bir şekilde arttığını gösterdi. Ek olarak, %5 F: %3 In eş katkılı ZnO filminin özdirenci en düşük seviyede, 1.65×10^{-1} Ωcm'de tespit edildi. Bu veriler, fotovoltaik hücreler, ekran teknolojileri ve LED'ler dahil olmak üzere gelişmiş opto-elektronik uygulamalar için %5 F: %3 In eş-katkılı ZnO filmlerinin potansiyelini ortaya koymaktadır. ZnO filmlerinin flor ve indiyumla eş-katkılanması, elektriksel ve optik özellikleri geliştirmek için umut verici bir strateji olarak ortaya çıkmaktadır.

*Corresponding author, e-mail: ibrahimgunes@comu.edu.tr
DOI: 10.29109/gujsc.1622733

1. INTRODUCTION (GİRİŞ)

Transparent conductive oxides (TCOs) play a critical role in numerous optoelectronic applications, such as photovoltaic devices, high-resolution displays, and LED technologies. Among TCO materials, indium tin oxide (ITO) is the most widely used, thanks to its exceptional combination of high optical transmittance (~90%) and extremely low electrical resistivity (~10^{-4} Ωcm) [1]. Despite these outstanding properties, the limited availability, high cost, and environmental issues associated with indium have driven the search for alternative materials to replace ITO. In this context, zinc oxide (ZnO) has emerged as a promising candidate due to its affordability, environmental friendliness, and comparable opto-electronic performance to other alternatives.

ZnO, with its wide bandgap (~3.3 eV), is an n-type semiconductor known for its excellent optical transparency in the visible spectrum [2]. However, the electrical conductivity of undoped ZnO is inferior to that of ITO, primarily because its carrier concentration ranges from 10^{17} to 10^{19} cm^{-3}, whereas ITO typically achieves ~10^{21} cm^{-3} [3]. This limitation reduces its practicality in TCO applications. To overcome this limitation, doping ZnO with group III elements such as aluminum (Al), gallium (Ga) or indium (In) has been widely investigated [4,5]. These dopants replace Zn^{2+} ions in the lattice, introducing extra electrons and increasing the carrier concentration [6]. Notably, In^{3+} ions (ionic radius: 0.80 Å) are closer in size to Zn^{2+} ions (ionic radius: 0.74 Å) than Al^{3+} (0.53 Å) or Ga^{3+} (0.61 Å) ions, minimizing lattice distortion and potentially enhancing carrier mobility [7]. However, excessive doping levels can lead to lattice strain and ionized impurity scattering, which limit electron mobility. Moreover, an overabundance of free carriers may result in increased absorption, thereby compromising optical transmittance [8]. Therefore, increasing the carrier concentration as well as mobility is important to improve the electrical properties of TCOs while maintaining their optical performance [2]. Recent research has revealed that co-doping ZnO with multiple elements –both cationic (e.g., Al, Ga, In) and anionic (e.g., fluorine (F), chlorine (Cl))– can significantly improve its opto-electronic properties [6,9–11]. Fluorine doping, in particular, offers unique advantages. In this context, the F doping enables the F^- ion to substitute in the ZnO lattice with minimal lattice distortion due to its ionic radius (1.31 Å) being quite similar to that of O^{2-} ion (1.35 Å) [7]. Furthermore, F doping can effectively passivate oxygen vacancies, reduce defect scattering, and enhance electron mobility while maintaining high optical transparency [12].

In previous studies, doped/co-doped ZnO films have been synthesized using vacuum-requiring techniques such as DC/RF magnetron sputtering [9,10] and pulsed laser deposition [5] as well as non-vacuum-requiring techniques such as sol-gel [13] and spray pyrolysis [14–16]. For example, Nguyen et al. utilized DC magnetron sputtering to fabricate F:In co-doped ZnO (FIZO) films, reporting substantial improvements in both electrical and optical properties [8]. Their findings demonstrated that F doping enhanced crystallinity, reduced lattice defects (e.g., V_{Zn}, O_{Zn}, V_O^{++}), and increased carrier concentration by 17-fold, along with a two-fold increase in mobility. In the same study, it was determined that FIZO films reached the lowest resistivity value of 5.24×10^{-4} Ωcm with an optical transmittance of 82%, highlighting their potential for TCO applications [8]. In another investigation, the sol-gel method was employed to synthesize ZnO thin films co-doped with fluorine and indium [13]. Analysis of XRD patterns showed a strong preference for the (002) crystal plane, while SEM imaging displayed nanofiber structures around 500 nm in size. Increasing the doping levels of F and In narrowed the optical band gap from 3.35 eV to 3.24 eV and reduced visible-light transparency from 75% to 60.8% [13]. In another study by Hadri et al., undoped ZnO, In doped ZnO (IZO) and F:In co-doped ZnO (FIZO) thin films were synthesized by chemical spray pyrolysis technique at 350 °C and the effect of F doping on some physical properties was investigated [14]. Their findings revealed that the (002) peak was dominant in XRD patterns, and the (101) peak intensity increased with higher F concentrations. The co-doped films exhibited 80% optical transparency within the 400–800 nm wavelength range, alongside a resistivity of 6.3×10^{-3} Ωcm, and their electrical properties improved significantly following annealing. These results underscore the potential of FIZO films for advanced opto-electronic applications, particularly in solar cells and display technologies [14]. Therefore, co-doping ZnO with both cationic and anionic dopants offer significant advantages: Group III cations (e.g., In^{3+}) contribute free electrons, while anions such as F^- can passivate defects and reduce scattering centers, thereby enhancing mobility. Additionally, the deposition technique plays a crucial role in minimizing production costs and improving the scalability of TCO technologies. From this perspective, the spray pyrolysis technique is particularly appealing as a thin-film deposition method due to its non-vacuum nature, low cost, capability for large-area coating, and ease of control

over experimental parameters. These advantages make spray pyrolysis a widely preferred technique for preparing co-doped zinc oxide films. However, despite extensive research into various doping combinations, studies on the effects of F:In co-doping on the physical properties, particularly opto-electrical behaviors, remain limited. Moreover, to the best of our knowledge, only a few studies on this topic utilizing spray pyrolysis have been reported in the literature [13,14,17].

In this research, ZnO films, including undoped, 3% In-doped, and 5% F:3% In co-doped samples, were synthesized via the ultrasonic spray pyrolysis (USP) technique. The study focuses on analyzing the physical properties of these films in detail through a co-doping approach. Specifically, this study aims to optimize the carrier concentration and mobility without compromising the optical transmittance. As a result, the obtained data provide an experimental basis for the development of F:In co-doped ZnO films based opto-electronic devices.

2. MATERIALS AND METHODS (MATERYAL VE METOD)

2.1. Deposition of Films (Filmlerin Biriktirilmesi)

In this research, zinc oxide films with undoped, indium-doped and fluorine-indium co-doped were synthesized via USP. Firstly, the microscope glass substrates used for film deposition were cleaned. The process was carried out by ultrasonicating with detergent solution, deionized (DI) water, acetone and methanol for 10 min each, followed by rinsing in DI water after each step. After the cleaning process, the substrates were carefully dried in an oven, and the film deposition process was subsequently conducted in two distinct stages. In the first stage, in order to investigate the effect of indium doping on the physical properties of zinc oxide films, undoped and 3% indium doped films were prepared. Spraying solutions were prepared by dissolving 0.1 M indium (III) chloride ($InCl_3$; 98%, Sigma-Aldrich) as the indium source and 0.1 M zinc acetate dihydrate ($Zn(CH_3CO_2)_2{\cdot}2H_2O$; ≥99.5%, Merck) as the zinc source in DI water. The substrate temperature was determined as 400°C and the prepared spraying solutions were sprayed onto glass substrates at a flow rate of 5 ml/min for 25 minutes to obtain films. The spraying solution was converted into droplets in the range of 10-60 μm by means of an ultrasonic atomizer. During the second stage, co-doping with fluorine and indium was implemented to further augment the properties of ZnO films. Based on a comprehensive review of literature and prior experimental results, the doping levels were set at 3% for indium and 5% for fluorine. To prepare a new spray solution, zinc acetate dihydrate, indium chloride, and ammonium fluoride (NH_4F; ≥98%, Merck) were dissolved in DI water at 0.1 M. The deposition process was carried out under consistent conditions, maintaining the same substrate temperature and flow rate as in the initial stage. The deposited films were left to cool naturally and were made ready for the characterization process. The schematic diagram of the USP thin film deposition technique used in this study was presented in detail in our previous study [18]. For clarity throughout this study, the films were designated as follows: undoped ZnO was labeled as ZO, 3% indium-doped ZnO as IZO, and 5% fluorine-indium co-doped ZnO as FIZO.

2.2. Characterization of Films (Filmlerin Karakterizasyonu)

The structural, surface and opto-electrical properties of the synthesized films were investigated by using various characterization techniques. Structural analyses were performed by using a PANalytical Empyrean XRD with CuK_α radiation (λ = 0.15405 nm) and XRD spectra taken in the 2θ range of 20°–80°. For the investigation of surface morphology and roughness, a Park Systems XE 100 AFM operating in non-contact mode was used. The average surface roughness (R_a) was calculated by XEI software over the scans of 5×5 μm² area. For morphological analysis, surface and cross-sectional images were obtained by a HITACHI SU5000 FE-SEM; at the same time, EDS spectra were taken to evaluate the elemental composition. Furthermore, the cross-sectional images provided the determination of the film thicknesses. Optical analyses were determined with Rigol Ultra-3660 spectrophotometer capable of measuring in the wavelength range of 300–1000 nm, while electrical analyses were evaluated by Hall effect measurements using Nanomagnetics ezHEMS system.

3. RESULTS (BULGULAR)

The structural features of the ZO, IZO, and FIZO films were evaluated based on their XRD patterns, as illustrated in Figure 1. A series of diffraction peaks were detected, primarily within the 2θ range of 20° to 80°, with notable positions near 32.2°, 34.8°, and 36.6°, among others. When compared with the standard data provided by ICDD File No: 36-1451, these peaks were identified as belonging to characteristic crystal planes of hexagonal ZnO, including (100), (002), and (101). Additionally, all peaks in the XRD patterns belong to the ZnO phase,

with no diffraction peaks corresponding to any secondary phases that might result from the dopant atoms. Therefore, In and F dopant atoms may have occupied the zinc or oxygen positions in the zinc oxide crystal structure or be trapped in amorphous regions at grain boundaries [19]. Previous studies have reported that F dopant atoms tend to localize at grain boundaries and surfaces with a high density of dangling bonds, where they can passivate these bonds [20]. As expected, the doped films displayed diffraction features corresponding to the ZnO crystal planes (100), (002), and (101). Slight shifts in the 2θ positions of these peaks were identified, attributed to the effects of doping. As listed in Table 1, the 2θ angles for these planes shifted to lower values in In-doped IZO films, while in F:In co-doped FIZO films, the angles shifted back to higher values. According to Bragg's law ($d = \lambda/2\sin\theta$), this indicates that the interplanar distance (d) initially increases with In doping in IZO films and then decreases again with F:In co-doping in FIZO films. Therefore, the shift of 2θ to lower angles in the IZO film is due to the larger ionic radius of In^{3+} (0.80 Å) than the ionic radius of Zn^{2+} (0.74 Å), supporting the successful incorporation of In ions into the Zn position [7]. On the other hand, the shift of 2θ to low angles in the FIZO film is due to the fact that the ionic radius of F^- ion (1.31 Å) is slightly smaller than the ionic radius of O^{2-} ion (1.35 Å), indicating that F ions successfully injected into the O positions [7]. These observations are consistent with a recent study by Nguyen et al., which reported similar changes in structural parameters upon doping [8].

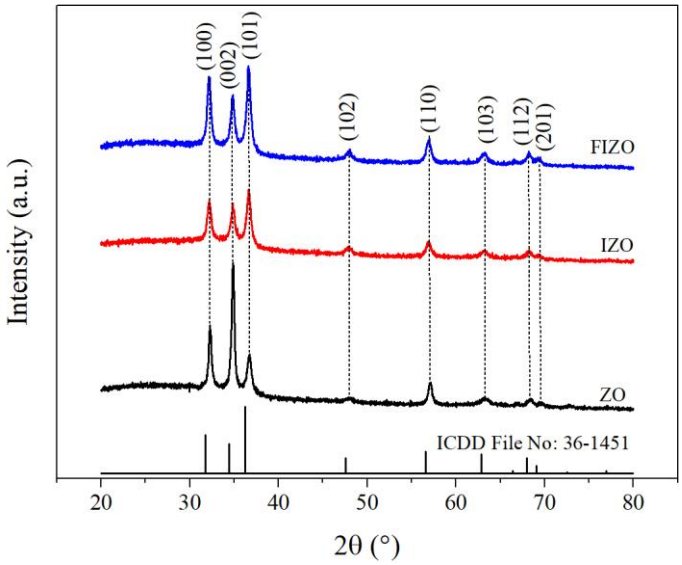

Figure 1. XRD patterns of the deposited ZO, IZO and FIZO films (Biriktirilen ZO, IZO ve FIZO filmlerine ait XRD desenleri)

Table 1 presents the structural parameters obtained from the XRD patterns. For the calculations of the texture coefficients (TC), crystallite size (D), micro-strain (ϵ), lattice constants in hexagonal crystal structure (a and c) and unit cell volume (V) of all deposited films, the well-known equations: $TC = (I/I_0)/[1/N(\sum I/I_0)]$, $D = K\lambda/\beta cos\theta$, $\varepsilon = \beta cot\theta/4$, $1/d^2 = 4/3\,[(h^2 + hk + k^2)/a^2] + (l^2/c^2)$, and $V = \sqrt{3}/2(a^2c)$ were used, respectively [21,22]. From the terms in these equations: I represent the intensity of the specific diffraction peak, while I_0 denotes the reference intensity obtained from the ICDD database. The total count of diffraction peaks is indicated by N. The shape factor, symbolized as K, is assigned a value of 0.94. The X-ray wavelength is expressed by λ, and full width at half maxima is referred to as β (measured in radians). Additionally, the Bragg angle is denoted by θ (in radians), and the crystallographic directions are represented by the Miller indices h, k, l.

As seen in Table 1, the ZO film exhibits the highest TC value (1.99) for the (002) plane, indicating that the crystals tend to grow along the c-axis perpendicular to the substrate surface preferential orientation. In contrast, IZO and FIZO films display lower TC values (1.04/1.22 and 1.16/1.10 for the (100)/(002) orientations, respectively), suggesting dominant growth along these planes and higher micro-strain, indicative of deformation in the crystal structure. Particularly in the IZO film, the (100) plane exhibits a broader β value (0.5402°), smaller crystallite size (16.0 nm), and higher micro-strain (8.17×10^{-3}). A study by Tubtimtae and Lee attributed the adverse effects on crystallinity in ZnO

films with high In doping concentrations (≥2%) to increased stress caused by the ionic radius mismatch between Zn^{2+} and In^{3+} [23]. In the FIZO film, while F doping positively influences the crystallinity of the IZO film, the crystallite sizes (ranging between 17.5–19.0 nm) are smaller, and microstrain values (6.04×10^{-3} to 7.43×10^{-3}) are relatively higher compared to the ZO film, indicating a lower crystallinity level. These results suggest that F doping partially stabilizes the lattice structure of the IZO film, leading to improved crystallinity. On the other hand, previous studies reported that Al doping in ZnO films significantly alters crystallite sizes due to the ionic radius difference between Al and Zn, whereas F doping causes less pronounced changes in crystallite size due to the similarity between the ionic radii of F^- and O^{2-} [6]. In conclusion, the XRD results indicate that F and In dopant atoms not only successfully integrate into the ZnO lattice but also alter lattice parameters and crystal structure characteristics. Furthermore, it can be inferred that F doping in the F:In co-doped film partially enhances the crystalline order and reduces crystal defects compared to the In-doped film. These results reveal that F:In co-doping is a potential tool to improve the structural properties of ZnO-based films.

Table 1. Key parameters obtained from the structural analysis of the deposited ZO, IZO, and FIZO films
(Biriktirilen ZO, IZO ve FIZO filmlerinin yapısal analizinden elde edilen temel parametreler)

Material	2θ (°)	d (Å)	hkl	β (°)	TC	D (nm)	ε×10^{-3}	a (Å)	c (Å)	c/a	V (Å^3)
ZO	32.27	2.7714	(100)	0.4027	0.77	21.4	6.07	3.212	5.143	1.601	45.98
	34.85	2.5719	(002)	0.4012	1.99	21.6	5.57				
	36.69	2.4473	(101)	0.4790	0.24	18.2	6.30				
IZO	32.17	2.7796	(100)	0.5402	1.04	16.0	8.17	3.219	5.146	1.598	46.19
	34.83	2.5734	(002)	0.5151	1.22	16.9	7.16				
	36.62	2.4513	(101)	0.4714	0.74	18.5	6.21				
FIZO	32.27	2.7714	(100)	0.4929	1.16	17.5	7.43	3.213	5.144	1.600	46.00
	34.85	2.5719	(002)	0.4699	1.10	18.5	6.53				
	36.68	2.4478	(101)	0.4590	0.74	19.0	6.04				

Surface morphology alterations in ZO, IZO, and FIZO films were analyzed using AFM images, as shown in Figure 2. From the AFM images, it can be observed that all films exhibit nearly homogeneous surfaces. Additionally, the bright and dark regions observed across the surfaces correspond to peaks and valleys, respectively, indicating the presence of randomly distributed particles of varying sizes on the surface. During the spraying process using an ultrasonic nozzle, droplet sizes ranging between 10–60 µm contribute to such irregularities on the film surfaces. As indicated in Table 2, the average surface roughness (R_a) of ZO, IZO, and FIZO films was measured to be 13.5 nm, 8.6 nm, and 10.9 nm, respectively. The roughness values indicate that the ZO film has a rougher surface than the other films, while indium doping significantly reduces surface roughness and results in a more uniform structure. However, in the F:In co-doped film, surface roughness increased again. The variations in surface roughness can be correlated with differences in crystallite sizes (ZO= ~22 nm, IZO= ~17 nm, FIZO= ~19 nm). Generally, films with rougher surfaces, such as ZO, tend to have larger crystallites due to reduced grain boundary density, which allows grains to expand more easily. In contrast, the smoother morphology observed in IZO films suggests that grain growth is more constrained, likely due to the lattice strain induced by indium, which restricts atomic mobility. In F:In co-doped films, the slight increase in roughness compared to IZO indicates partial strain relaxation facilitated by fluorine incorporation, leading to a moderate increase in crystallite size.

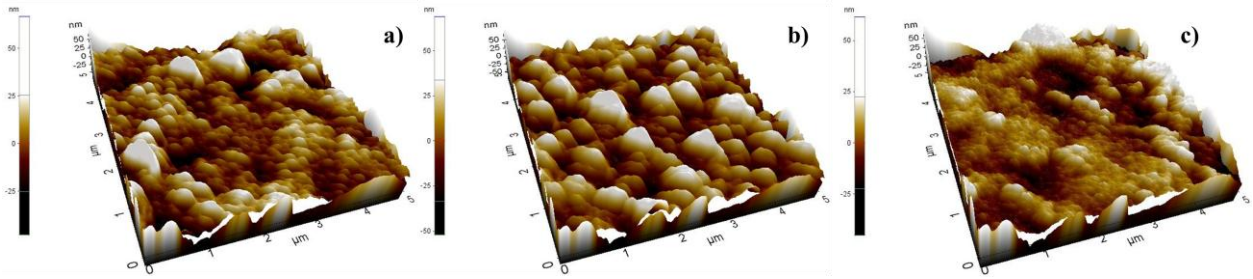

Figure 2. 3D-AFM images of the deposited films: **(a)** ZO, **(b)** IZO, and **(c)** FIZO (Biriktirilen filmlere ait 3D-AFM görüntüleri: **(a)** ZO, **(b)** IZO ve **(c)** FIZO)

Figure 3 shows SEM images taken at 100kX magnification, providing additional insights into the surface textures of the deposited films alongside the AFM results. These SEM images confirm that the films exhibit a nanoparticle-like, homogeneous, and compact structure without any visible voids or cracks across the surface. In ZO films, a surface morphology consisting of randomly oriented grains as well as regular and distinctly plate-like structures is observed. In IZO and FIZO films, it is observed that both In doping and F:In co-doping clearly change the surface morphology and show a transition from plate-like morphology to granular nanostructures. Comparable results for indium doped zinc oxide films fabricated by spray pyrolysis have been highlighted in previous research by Bharath et al. [24]. Additionally, film thicknesses were calculated by averaging five different regions of the cross-sectional images given in Figure 3 using the ImageJ program. The inset cross-sectional SEM images further illustrate the dense and continuous structure of the films, with no visible gaps or irregularities at the substrate-film interface. These images also confirm that the films maintain uniform thickness across different regions, supporting the accuracy of the thickness measurements. The results indicate that the average thicknesses of the ZO, IZO, and FIZO films were 1.08 µm, 1.21 µm, and 1.28 µm, respectively. The findings indicate that the inclusion of dopant atoms increases the film growth rate, resulting in thicker films.

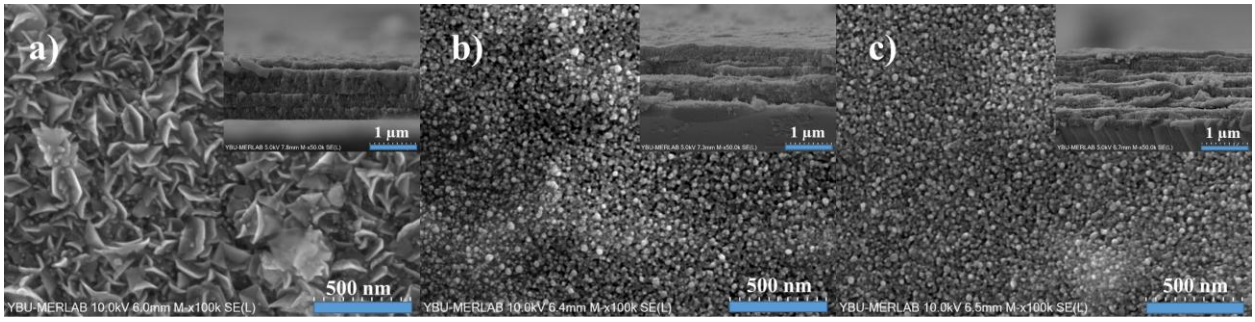

Figure 3. SEM surface images at 100kX magnification and cross-sectional SEM images at 50kX magnification (inset) of the deposited films: **(a)** ZO, **(b)** IZO, and **(c)** FIZO (Biriktirilen filmlere ait 100kX büyütmeli SEM yüzey görüntüleri ve 50kX büyütmeli kesitsel SEM görüntüleri (içine yerleştirilen): **(a)** ZO, **(b)** IZO ve **(c)** FIZO)

Figure 4 presents the EDS spectra obtained to perform elemental analysis of the deposited films. As anticipated, strong signals corresponding to zinc and oxygen elements were detected in all the films. In the ZO film, the atomic percentages of zinc and oxygen were measured at 52.2% and 47.8%, respectively. In the IZO film, the atomic percentage of In was determined to be 1.9%. For the F:In co-doped FIZO films, the dopants were successfully detected, with atomic percentages of In and F measured at 1.0% and 0.6%, respectively. Moreover, the ratios of zinc and oxygen elements in all films were found to closely align with the stoichiometric composition. Despite the low concentrations of the dopant elements, their successful incorporation into the films was confirmed. The low incorporation of In and F into ZnO films is primarily due to the inherent limitations of the spray pyrolysis process. The volatility of precursor compounds, incomplete thermal decomposition, and diffusion rate differences can reduce dopant retention in the film. Fluorine, being highly volatile, may partially evaporate before integrating into the ZnO lattice, while indium incorporation is constrained by its solubility limit in ZnO. Despite these factors, the successful detection of dopants confirms their presence in the film structure.

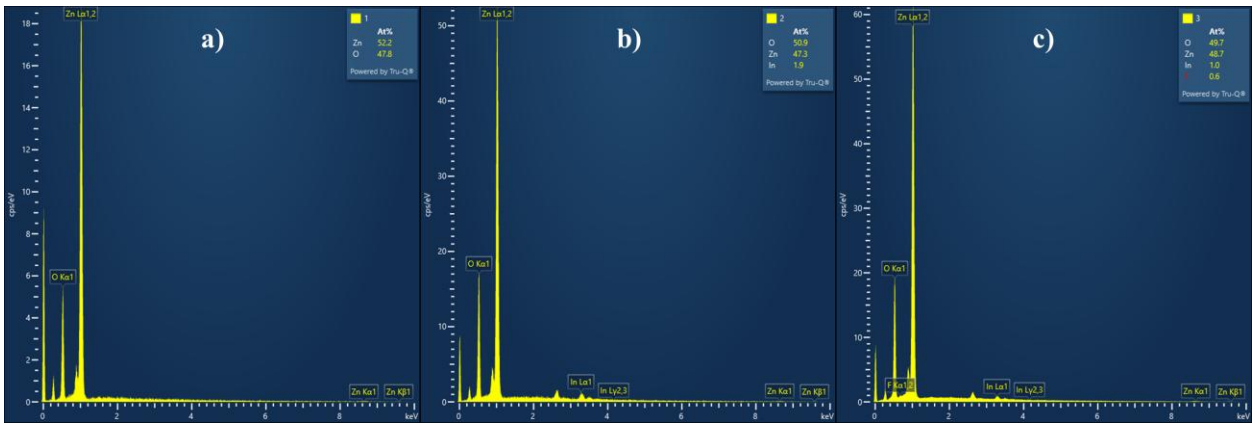

Figure 4. EDS spectra of the deposited films: **(a)** ZO, **(b)** IZO, and **(c)** FIZO (Biriktirilen filmlere ait EDS spektrumları: **(a)** ZO, **(b)** IZO ve **(c)** FIZO)

In Figure 5, optical transmittance spectra of the deposited ZO, IZO, and FIZO films are given, demonstrating that each film maintains a transmittance of at least 80% across the visible spectrum. According to Table 2, the undoped ZO film exhibited an average transmittance of around 84% within the visible wavelength range. However, this value decreased to ~80% with In doping (IZO) and then increased to ~83% with F:In co-doping (FIZO). This variation in transmittance may be attributed to light scattering at grain boundaries, which can occur because of doping. Studies conducted previously have noted comparable trends in similar contexts [14,24].

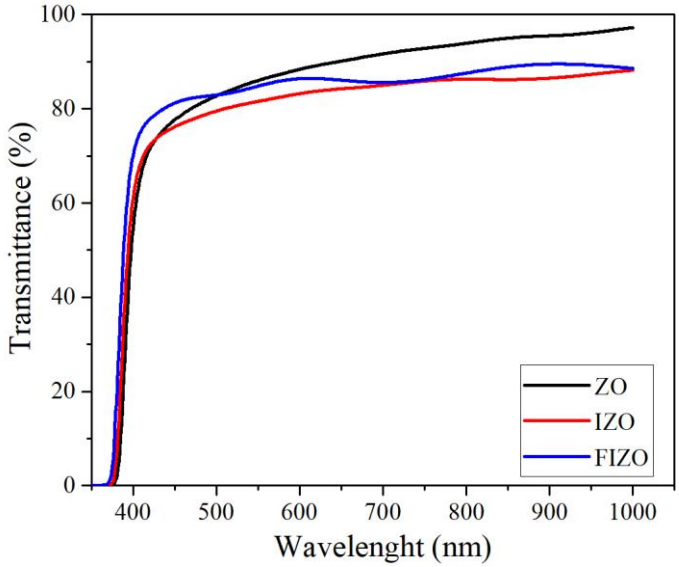

Figure 5. Transmittance spectra belonging to the deposited ZO, IZO, and FIZO films (Biriktirilen ZO, IZO ve FIZO filmlerine ait geçirgenlik spektrumları)

The optical band gap values of the deposited films were determined using the well-known Tauc method. This method, depicted in the $(\alpha h\nu)^2$ versus $h\nu$ graphs in Figure 6(a–c), relies on the relationship given by $(\alpha h\nu)^2 = K(h\nu - E_g)$. In this equation, α denotes the absorption coefficient, $h\nu$ is the photon energy, K is a proportionality constant, and E_g is the optical band gap. Table 2 summarizes the optical band gap values obtained through this method, showing 3.23 eV, 3.28 eV, and 3.32 eV for ZO, IZO, and FIZO films, respectively. The observed band gap widening in the IZO film is likely a consequence of the increased carrier concentration, which induces the Burstein-Moss effect—a phenomenon that will be further examined in the electrical analysis section. The band gap widening is more pronounced in the FIZO films, which is due to the additional free electrons introduced by F doping, further enhancing this effect. Moreover, the results align with data from prior studies, which have also observed an increase in the optical band gap when ZnO films are doped with In or co-doped with F:In [15,25,26]. Such band gap expansion is typically linked to the Burstein-Moss effect, as noted in earlier works [15,19,25]. In addition, localized states may occur within the band gap due to crystal defects or doping atoms, and this may lead to sagging at the band edges. The Urbach energy (E_U

), which reflects the extent of band tailing at the band edges, was calculated from the slope of the lnα versus $h\nu$ plot shown in Figure 6(d–f). This calculation utilizes the well-known relationship $\alpha_0 exp(h\nu/E_U)$, where α_0 is a constant. Urbach energy values were calculated as 75 meV, 82 meV and 79 meV for ZO, IZO and FIZO films, respectively (Table 2). In this context, it has been observed that neither In doping nor F:In co-doping leads to substantial changes in the electronic band irregularities of ZnO films. The slight increase in Urbach energy, on the other hand, can likely be attributed to the dopant-induced defect density, which contributes to structural disorder and enhanced carrier interactions. This observation is corroborated by the micro-strain values obtained from XRD analysis The findings suggest that the optical properties of ZnO films are more effectively enhanced through the F:In co-doping process when compared to solely indium doping.

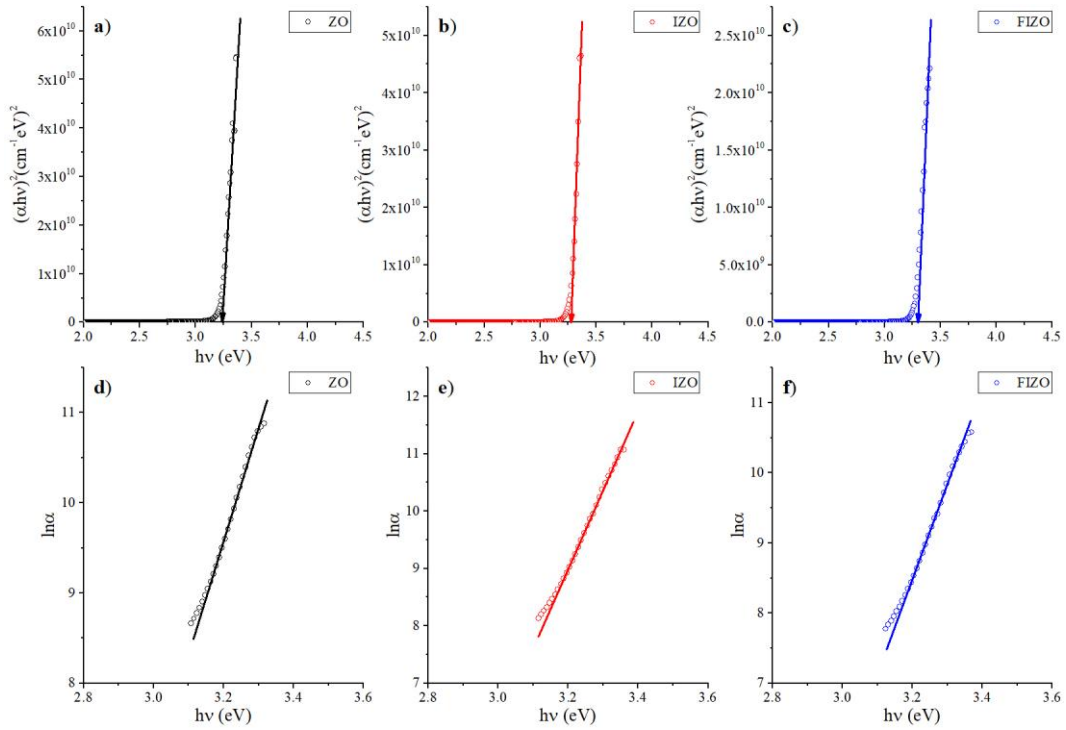

Fig. 6. (a-c) Tauc plots and **(d-f)** Urbach plots of the deposited ZO, IZO and FIZO films (Biriktirilen ZO, IZO ve FIZO filmlerine ait **(a-c)** Tauc grafikleri ve **(d-f)** Urbach grafikleri)

Electrical analyses of the deposited ZO, IZO and FIZO films were performed by taking Hall effect measurements. Table 2 shows electrical resistivity (ρ), sheet resistance (R_S), carrier concentration (N) and carrier mobility (μ) are summarized. In addition, Figure 7 shows the trends observed in these parameters for all deposited films. Hall effect analysis confirmed that all films exhibited *n*-type electrical conductivity. The *n*-type conductivity of undoped ZnO is well-documented in the literature and is attributed to donor defects such as oxygen vacancies (V_O) and zinc interstitials (Zn_i).

Table 2. Key parameters obtained from the optical and electrical analysis of the deposited ZO, IZO, and FIZO films **(**Biriktirilen ZO, IZO ve FIZO filmlerinin optik ve elektrik analizlerinden elde edilen temel parametreler)

Material	T (%)	E_g (eV)	E_U (meV)	ρ (Ωcm)	N (cm^{-3})	μ (cm^2/Vs)	R_S (Ω/sq)	FoM (Ω^{-1})
ZnO	84	3.23	75	2.02×10^{0}	1.03×10^{17}	29.18	1.87×10^{4}	9.35×10^{-6}
IZO	80	3.28	82	7.57×10^{-1}	3.17×10^{17}	12.35	6.26×10^{3}	1.72×10^{-5}
FIZO	83	3.32	79	1.65×10^{-1}	1.14×10^{18}	25.62	1.29×10^{3}	1.20×10^{-4}

As shown in Figure 7 and Table 2, the ZO film exhibits a resistivity of 2.02 Ωcm, a relatively low carrier concentration (1.03×10^{17} cm^{-3}), and a mobility of 29.18 $cm^2/V\cdot s$. The ZO films highest crystallite size (21.6 nm) and lowest micro-strain value (6.07×10^{-3}) observed in the XRD analysis indicate fewer electron scattering centers, supporting its higher mobility. However, the low carrier concentration limits its conductivity. In contrast, the IZO film shows a significant decrease in resistivity (0.757 Ωcm) due to an increase in carrier concentration to 3.17×10^{17} cm^{-3}. This

increase in carrier concentration is attributed to the substitution of Zn^{2+} ions with In^{3+} ions in the ZnO lattice, resulting in additional free electrons being introduced into the conduction band [15,27]. However, the mobility of the IZO film (12.35 cm^2/Vs) is lower compared to the ZO film. This reduction in mobility can be explained by the high micro-strain (8.17×10^{-3}) and smaller crystallite size (16.0 nm) observed in the IZO film, which increase electron scattering, as noted in Table 1. Furthermore, ionized impurity scattering, a phenomenon commonly observed in doped films due to high carrier densities, also contributes to the reduced mobility. In the literature, Kathwate et al. reported that at 4% In doping, the solubility limit of In in ZnO is reached, leading to the formation of scattering centers and an increase in resistivity [15]. However, in this study, a 3% In doping concentration resulted in a significant increase in carrier density and a decrease in resistivity. This implies that In ions are homogeneously distributed within the ZnO structure, enhancing conductivity rather than forming segregations at grain boundaries. Thus, the effects of micro-strain and carrier scattering appear to depend on the doping level and the distribution of ions within the ZnO structure. The FIZO film proves the best electrical performance, with the lowest resistivity (1.65×10^{-1} Ωcm) and the highest carrier concentration (1.14×10^{18} cm^{-3}). This improvement can be attributed to the substitution of Zn^{2+} ions by In^{3+} and O^{2-} ions by F^- in the ZnO lattice, creating additional donor defects [8,14,28]. Previous studies have reported that fluorine forms chemical bonds with Zn interstitials, reducing intrinsic defects and increasing carrier concentration [14,28]. Moreover, the mobility of the FIZO film (25.62 cm^2/Vs) is higher than that of the IZO film, which has a lower carrier density. This improvement is supported by fluorine's ability to passivate dangling bonds at grain boundaries, reduce electron scattering, and stabilize the crystal lattice by lowering micro-strain (7.43×10^{-3}) [14,28]. Additionally, fluorine's ability to slightly increase the crystallite size (17.5 nm) and promote a more homogeneous structure further enhances its positive impact on mobility.

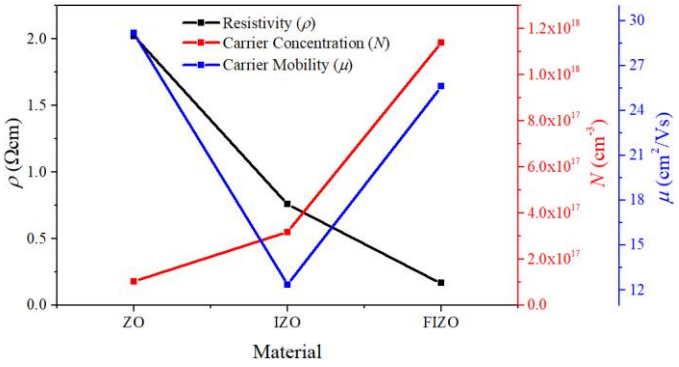

Figure 7. Variation graphs of electrical resistivity, carrier concentration and carrier mobility of the deposited ZO, IZO and FIZO films (Biriktirilen ZO, IZO ve FIZO filmlerine ait elektriksel özdirenç, taşıyıcı konsantrasyonu ve taşıyıcı mobilitesi değişim grafikleri)

The figure of merit (FoM; ϕ) value used in the evaluation of the usability of the material as TCO and suggested by Haacke [29] was calculated in accordance with the equation $\phi = T^{10}/R_S$. Here, T is the average transmittance in the range of 400-700 nm and R_S represents the sheet resistance. The sheet resistance values were determined as 1.87×10^4 Ω/sq in the ZO film, 6.26×10^3 Ω/sq in the IZO film and 1.29×10^3 Ω/sq in the FIZO film. In this context, according to Table 2, FIZO films show the highest FoM value at 1.20×10^{-4} Ω^{-1}, with IZO and ZO films following at 1.72×10^{-5} Ω^{-1} and 9.35×10^{-6} Ω^{-1}, respectively. While the IZO films demonstrated improved performance compared to ZnO in terms of FoM, the FIZO film produced the best result, making it the most suitable for opto-electronic applications. These results indicate that F:In co-doping significantly improves the electrical performance of ZnO films. The FIZO films exhibit the highest carrier density, lowest resistivity, lowest sheet resistance, and highest FoM value, effectively combining superior opto-electrical properties. The findings emphasize the potential of FIZO films in opto-electronic technologies, with specific applications in energy harvesting and display systems.

4. CONCLUSIONS (SONUÇLAR)

In this study, the effect of F:In co-doping strategy on the physical properties of ZnO films was investigated comprehensively. The results reveal that the co-doping approach has significant changes on both structural and opto-electronic properties. Structural analyses revealed that F:In co-doping stabilizes the ZnO crystal structure and reduces

crystal defects compared to In doping alone. Morphological analyses showed that FIZO films exhibit granular nanostructures and decreased surface roughness compared to undoped ZO films. In electrical analyses, it was found that the carrier concentration in FIZO films increased approximately 11-fold and reached 1.14×10^{18} cm^{-3}, and the electrical resistivity decreased to the lowest level of 1.65×10^{-1} Ωcm. This improvement is attributed to F doping, which passivates oxygen vacancies and enhances carrier mobility, thereby reducing electron scattering in the ZnO structure. Optical analyses wrote down that FIZO films optimize opto-electronic performance by achieving high transparency (~83%) and relatively low sheet resistance (1.29×10^{3} Ω/sq). The calculated figure of merit (FoM) value of 1.20×10^{-4} Ω^{-1} confirms that FIZO films deliver the best performance for opto-electronic devices. In conclusion, this study provides a significant scientific foundation for the potential use of FIZO films in technologies such as photovoltaic devices, high-resolution displays, and LEDs. The findings highlight the promise of F:In co-doped ZnO films deposited via the USP technique—a rarely studied approach in the literature—for low-cost, high-performance transparent conductive electrodes and other opto-electronic applications.

ACKNOWLEDGMENTS (TEŞEKKÜR)

I would like to thank Assoc. Prof. Dr. Emrah SARICA, faculty member of the Electrical and Electronics Engineering Department of Başkent University, for providing laboratory facilities and support in conducting the Hall effect measurements.

Hall etkisi ölçümlerinin gerçekleştirilmesinde sağladığı laboratuvar imkânları ve desteği için, Başkent Üniversitesi Elektrik-Elektronik Mühendisliği Bölümü öğretim üyesi Doç. Dr. Emrah Sarıca'ya, teşekkürlerimi sunarım.

DECLARATION OF ETHICAL STANDARDS (ETİK STANDARTLARIN BEYANI)

The author of this article declares that the materials and methods they use in their work do not require ethical committee approval and/or legal-specific permission.

Bu makalenin yazarı çalışmalarında kullandıkları materyal ve yöntemlerin etik kurul izni ve/veya yasal-özel bir izin gerektirmediğini beyan ederler.

AUTHORS' CONTRIBUTIONS (YAZARLARIN KATKILARI)

***Ibrahim GUNES*:** He conducted the experiments, analyzed the results and performed the writing process.

Deneyleri yapmış, sonuçlarını analiz etmiş ve makalenin yazım işlemini gerçekleştirmiştir.

CONFLICT OF INTEREST (ÇIKAR ÇATIŞMASI)

There is no conflict of interest in this study.

Bu çalışmada herhangi bir çıkar çatışması yoktur.

REFERENCES (KAYNAKLAR)

[1] A.H. Ali, Z. Hassan, A. Shuhaimi, Enhancement of optical transmittance and electrical resistivity of post-annealed ITO thin films RF sputtered on Si, Appl. Surf. Sci. 443 (2018) 544–547.

[2] H. Liu, H. Li, J. Tao, J. Liu, J. Yang, J. Li, J. Song, J. Ren, M. Wang, S. Yang, X. Song, Y. Wang, Single Crystalline Transparent Conducting F, Al, and Ga Co-Doped ZnO Thin Films with High Photoelectrical Performance, ACS Appl. Mater. Interfaces. 15 (2023) 22195–22203.

[3] Ü. Özgür, Y.I. Alivov, C. Liu, A. Teke, M.A. Reshchikov, S. Doğan, V. Avrutin, S.J. Cho, H. Morkoç, A comprehensive review of ZnO materials and devices, J. Appl. Phys. 98 (2005) 1–103.

[4] H. Benali, B. Hartiti, F. Lmai, A. Batan, S. Fadili, P. Thevenin, Synthesis and characterization of Al-doped ZnO thin-films for photovoltaic applications, Mater. Today Proc. (2024).

[5] R.S. Ajimsha, A.K. Das, P. Misra, M.P. Joshi, L.M. Kukreja, R. Kumar, T.K. Sharma, S.M. Oak, Observation of low resistivity and high mobility in Ga doped ZnO thin films grown by buffer assisted pulsed laser deposition, J. Alloys Compd. 638 (2015) 55–58.

[6] K.M. Kang, Y. Wang, M. Kim, C. Lee, H.H. Park, Al/F codoping effect on the structural, electrical, and optical properties of ZnO films grown via atomic layer deposition, Appl. Surf. Sci. 535 (2021) 147734.

[7] B.Y.R.D. Shannon, M. H, N.H. Baur, O.H. Gibbs, M. Eu, V. Cu, Revised Effective Ionic Radii and Systematic Studies of Interatomie

Distances in Halides and Chaleogenides, Acta Cryst. A32 (1976) 751–767.

[8] T.H. Nguyen, A.T.T. Pham, T.N. Le Pham, T.M. Le, T.T. Duong, D. Van Hoang, K.D. Nguyen, T.D.T. Ung, T.B. Phan, V.C. Tran, Co-doping effects of fluorine and indium on ZnO transparent electrode films, Ceram. Int. 50 (2024) 16698–16703.

[9] G. Zheng, J. Song, J. Zhang, J. Li, B. Han, X. Meng, F. Yang, Y. Zhao, Y. Wang, Investigation of physical properties of F-and-Ga co-doped ZnO thin films grown by RF magnetron sputtering for perovskite solar cells applications, Mater. Sci. Semicond. Process. 112 (2020) 105016.

[10] F.H. Hsu, N.F. Wang, Y.Z. Tsai, M.C. Chuang, Y.S. Cheng, M.P. Houng, Study of working pressure on the optoelectrical properties of Al-Y codoped ZnO thin-film deposited using DC magnetron sputtering for solar cell applications, Appl. Surf. Sci. 280 (2013) 104–108.

[11] G. V. Colibaba, D. Rusnac, V. Fedorov, P. Petrenko, E. V. Monaico, Low-temperature sintering of highly conductive ZnO:Ga:Cl ceramics by means of chemical vapor transport, J. Eur. Ceram. Soc. 41 (2021) 443–450.

[12] Y.J. Choi, K.M. Kang, H.H. Park, Anion-controlled passivation effect of the atomic layer deposited ZnO films by F substitution to O-related defects on the electronic band structure for transparent contact layer of solar cell applications, Sol. Energy Mater. Sol. Cells. 132 (2015) 403–409.

[13] E.F. Keskenler, G. Turgut, S. Doğan, Investigation of structural and optical properties of ZnO films co-doped with fluorine and indium, Superlattices Microstruct. 52 (2012) 107–115.

[14] A. Hadri, M. Taibi, M. Loghmarti, C. Nassiri, T. Slimani Tlemcąni, A. Mzerd, Development of transparent conductive indium and fluorine co-doped ZnO thin films: Effect of F concentration and post-annealing temperature, Thin Solid Films. 601 (2016) 7–12.

[15] L.H. Kathwate, V.D. Mote, Optical and Electrical Properties of In-doped ZnO Films via the Spray Pyrolysis Technique for Optoelectronics Device Applications, J. Electron. Mater. 51 (2022) 6894–6902.

[16] I. Gunes, E. Sarica, V. Bilgin, Enhancing Physical Properties: Chromium-Doped Zinc Oxide Thin Films Deposited by Ultrasonic Spray Pyrolysis, Tekirdag Namik Kemal Univ. Inst. Nat. Appl. Sci. 2 (2023) 62–70.

[17] O.G. Morales-Saavedra, L. Castañeda, J.G. Bañuelos, R. Ortega-Martínez, Morphological, optical, and nonlinear optical properties of fluorine-indium-doped zinc oxide thin films, Laser Phys. 18 (2008) 283–291.

[18] I. Gunes, Enhancing π-SnS thin films and fabrication of p-SnS/n-Si heterostructures through flow rate control in ultrasonic spray pyrolysis for improved photovoltaic performance, Appl. Phys. A. 130 (2024) 574.

[19] F. Yang, J. Song, X. Chen, X. Lu, J. Li, Q. Xue, B. Han, X. Meng, J. Li, Y. Wang, Ultrasonic spray pyrolysis-induced growth of highly transparent and conductive F, Cl, Al, and Ga co-doped ZnO films, Sol. Energy. 228 (2021) 168–174.

[20] T.H. Huang, P.K. Yang, D.H. Lien, C.F. Kang, M.L. Tsai, Y.L. Chueh, J.H. He, Resistive memory for harsh electronics: Immunity to surface effect and high corrosion resistance via surface modification, Sci. Rep. 4 (2014) 1–5.

[21] S.S. Shinde, P.S. Shinde, S.M. Pawar, A. V. Moholkar, C.H. Bhosale, K.Y. Rajpure, Physical properties of transparent and conducting sprayed fluorine doped zinc oxide thin films, Solid State Sci. 10 (2008) 1209–1214.

[22] B.D. Cullity, Elements of X-Ray Diffraction, Addison-Wesley Publishing Company, Inc., 1956.

[23] A. Tubtimtae, M.W. Lee, ZnO nanorods on undoped and indium-doped ZnO thin films as a TCO layer on nonconductive glass for dye-sensitized solar cells, Superlattices Microstruct. 52 (2012) 987–996.

[24] S.P. Bharath, K. V. Bangera, G.K. Shivakumar, Enhanced gas sensing properties of indium doped ZnO thin films, Superlattices Microstruct. 124 (2018) 72–78.

[25] P. Dhamodharan, J. Chen, C. Manoharan, Fabrication of In doped ZnO thin films by spray pyrolysis as photoanode in DSSCs, Surfaces and Interfaces. 23 (2021) 100965.

[26] T. V. Vimalkumar, N. Poornima, K.B. Jinesh, C.S. Kartha, K.P. Vijayakumar, On single doping and co-doping of spray pyrolysed ZnO films: Structural, electrical and optical characterisation, Appl. Surf. Sci. 257 (2011) 8334–8340.

[27] P. Nuthongkum, P. Yansakorn, K. Chongsri, R. Noonuruk, P. Junlabhut, Improvement of structural, optical and electrical properties of indium-doped ZnO nanoparticles synthesized by Co-precipitation method, J. Mater. Sci. Mater. Electron. 34 (2023) 1–10.

[28] A.T.T. Pham, N.M. Ngo, O.K.T. Le, D. Van Hoang, T.H. Nguyen, T.B. Phan, V.C. Tran, High-mobility sputtered F-doped ZnO films as good-performance transparent-electrode layers, J. Sci. Adv. Mater. Devices. 6 (2021) 446–452.

[29] G. Haacke, New figure of merit for transparent conductors *, J. Appl. Phys. 47 (1976) 4086–4089.